State relevance and modal analysis in electrical microgrids with 100% grid-forming converters

Andrés Tomás-Martín
IIT, ETSI ICAI
Comillas Pontifical University
Madrid, Spain
ORCID 0000-0003-2048-7197

Aurelio García-Cerrada
IIT, ETSI ICAI
Comillas Pontifical University
Madrid, Spain
ORCID 0000-0003-1950-2927

Lukas Sigrist
IIT, ETSI ICAI
Comillas Pontifical University
Madrid, Spain
ORCID 0000-0003-2177-2029

Sauro Yagüe
IQS Department of Industrial Engineering
Ramón Llull University
Barcelona, Spain
ORCID 0000-0002-0510-0698

Jorge Suárez-Porras
IIT, ETSI ICAI
Comillas Pontifical University
Madrid, Spain
ORCID 0000-0003-0001-8131

***Abstract*—In traditional power systems, dominated by synchronous generators, the separation between time scales is well-known due to the physical response of the generating units. However, the fast-growing deployment of renewable energy resources (RERs) is bringing an increasing number of generating units based on fast-acting electronic power converters to modern power systems. Nowadays, having an islanded portion of the grid with 100 % electronic generation, at least temporarily, is not unthinkable and, in this case, time-scale separation among dynamics would depend on control design and would not be straightforward. Therefore, the classical model-reduction approach neglecting the dynamics of fast-varying state variables is, at least, questionable. This paper proposes a method to identify relevant states in a modern power system in order to have an accurate input-output response description in any reduced-order model. The method is based on the modal analysis of a balanced realisation of the system (i.e., a linear transformation in which the transformed states' energies in the output response are known). The proposed method is illustrated on a microgrid with 100% grid-forming electronic power converters. Simulation results show that the proposed method can identify the system's relevant states even in cases with unclear time-scale separation.**

***Index Terms*—state relevance, modal analysis, microgrids, distributed secondary control**

Acronyms

HSV	Hankel singular value
HVDC	high-voltage direct-current
MOR	model order reduction
PCC	point of common coupling
RER	renewable energy resource
VSC	voltage-source converter
FACTS	flexible alternating current transmission system
RC	relevance coefficient

This work has been partially financed through the research program S2018/EMT-4366 PROMINT-CAM on Smart Grids of Madrid Government, Spain, with 50% support from the European Social Fund and by Grants RTI2018-098865-B-C31 and RTC-2017-6296-3 funded by MCIN/AEI/ 10.13039/501100011033 and by "ERDF A way of making Europe".

I. Introduction

Traditional power systems usually involve large synchronous machines for generation, e.g. nuclear or thermal power plants. These machines have large physical inertia due to their rotating mass, which allows the system to respond immediately to disturbances by absorbing or releasing kinetic energy. In this scenario, power system models can be easily split into slowly-varying electromechanical variables, e.g. voltage and speed of synchronous generators, and fast-varying electromagnetic variables, e.g. line currents and bus voltages [1]. With the development of renewable energy resources (RERs), usually interfaced by power electronics, future power systems are bound to have less physical inertia and, although there are ways to mimic the physical inertia of synchronous machines with electronic converters [2], [3], all of them are purely control techniques. Therefore, in the future, the time-scale separation in power systems will also depend on the control design and not only on the physical behaviour of the generating units. Clarifying the time-scale separation in power systems with RERs is essential for a model-order reduction [4].

Some studies in systems with power electronics still rely solely on the conventional assumptions of speed dynamics, i.e., neglecting the fastest control layers [5]. Ignoring power-line dynamics is a common practice in power systems. However, [6] already proposes the use of hybrid network models for small-signal stability analysis of power systems with fast-acting voltage-source converter (VSC)-based stations of high-voltage direct-current (HVDC) and/or flexible alternating current transmission systems (FACTSs), showing more accurate results. Similar studies with guidelines to select which dynamics to include in reduced-order models are applied to HVDC [7] and FACTS [8].

More recently, the work in [9] shows that complex AC-line models are necessary to study the dynamics of power systems with VSCs if high-frequency phenomena such as harmonic stability [10] or electromagnetic converter interactions [11] are to be addressed reliably.

The importance of each state in the dynamic response of a linear system is usually case-dependent. Guidelines on how to select the important states are based either on previous knowledge about power system dynamics or on eigenvalue and participation analysis. Since eigenvalues and participation factors do not depend on the choice of the system's inputs and outputs, this approach deserves further research.

In a balanced realisation of a linear system, the energy of each state variable in the input-output response of the system can be calculated using the so-called Hankel singular values (HSVs) [12]. Balanced realisations have been used before for model order reduction (MOR) in power systems [13], with good performance. However, the state variables of the balanced realisation are obtained from the original ones using a linear transformation and may not have physical meaning. A better insight into the system dynamics can be provided if the relevance in the input-output response of the physically-meaningful state variables of the system can be investigated as in [14]. This paper investigates the performance of that algorithm in a different scenario and clarifies the meaning of the results obtained.

The rest of the paper is organised as follows: Section II explains the algorithm for state-relevance calculation. Section III introduces the model used to describe a microgrid with 100% electronic generation with grid-forming VSCs. Section IV presents the distribution system used for a case study. Section IV-A shows the algorithm's performance in an ideal scenario, and Section IV-B shows the algorithm's performance in a system with an unusual time-scale separation among control layers. Section V concludes the paper.

II. Calculating state relevance

A linear system can always be transformed into another one whose states ($\overline{x}$) are a linear combination of the states of the original system (x) given by an invertible transformation matrix $\mathbf{T}$ such that $\overline{x} = \mathbf{T}x$ [12]. The original linear system is consequently transformed into:

$$\begin{cases} \dot{\overline{x}} = \mathbf{T}\mathbf{A}\mathbf{T}^{-1}\overline{x} + \mathbf{T}\mathbf{B}u \\ y = \mathbf{C}\mathbf{T}^{-1}\overline{x} + \mathbf{D}u \end{cases} \quad (1)$$

where the new controllability and observability Gramians are:

$$\overline{\mathbf{W}}_c^2 = \mathbf{T}\mathbf{W}_c^2\mathbf{T}^T \qquad \overline{\mathbf{W}}_o^2 = (\mathbf{T}^{-1})^T\mathbf{W}_o^2\mathbf{T}^{-1} \quad (2)$$

A balanced realisation in (1) means that:

$$\overline{\mathbf{W}}_c^2 = \overline{\mathbf{W}}_o^2 = diag(g_i) \quad (3)$$

where g_i are the HSVs. Small entries in g_i indicate states that can be removed to simplify the model since both their observability and controllability are small, whereas large entries indicate the most relevant states [15].

Since the balanced transformation is linear, the transformed system has the same eigenvalues as the original system; therefore, relevant eigenvalues of the transformed system will also be relevant eigenvalues of the original system. Relevant states of the transformed system can be chosen based on the values of g_i after the transformation in (1)-(3), and relevant eigenvalues can be determined by checking which eigenvalues have high participation factors in the relevant states of the balanced realisation. The mode-in-state participation factors normalised as in [16] (based on [17]) are used here:

$$p_{ji} = \frac{|w_{ij}|\,|v_{ji}|}{\sum_{\forall k}|w_{ik}|\,|v_{ki}|} \quad (4)$$

where p_{ji} is the normalised mode(i)-in-state(j) participation factor in a linear system, v_{ji} is the element of the $j-th$ row and $i-th$ column of matrix $\mathbf{V}$ of right column eigenvectors and w_{ij} is the element of the $i-th$ row and $j-th$ column of matrix $\mathbf{W}$ of left row eigenvectors calculated as $\mathbf{W} = \mathbf{V}^{-1}$.

The value of g_j can be used to weight $\bar{p}_{ij}$ as:

$$\hat{\mathbf{R}}_\lambda = [\hat{R}_\lambda(\lambda_1), \cdots, \hat{R}_\lambda(\lambda_n)]^T = \left([g_1, \cdots, g_n] \cdot \overline{\mathbf{P}}\right)^T \quad (5)$$

where $\hat{R}(\lambda_i)$ will be called the "relevance of eigenvalue λ_i" and $\overline{\mathbf{P}}$ is the participation matrix of the transformed system which has $\bar{p}_{ij}$ in its $i-th$ row and $j-th$ column. The bar above $\mathbf{P}$ and its elements has been used to indicate that they have been calculated using the balanced realisation in (1). Normalising yields:

$$\mathbf{R}_\lambda = [R_\lambda(\lambda_1), \ldots, R_\lambda(\lambda_n)]^T = \hat{\mathbf{R}}_\lambda / max(\hat{\mathbf{R}}_\lambda) \quad (6)$$

Let us now weigh each column of the participation matrix of the original system ($\mathbf{P}$) with the relevance of its associated eigenvalue ($\hat{R}(\lambda_i)$). By summing all these weighted columns, the resulting column vector can be used to quantify the "relevance of each state":

$$\hat{\mathbf{R}}_x = \mathbf{P} \cdot \mathbf{R}_\lambda \quad (7)$$

which can be normalised as follows:

$$\mathbf{R}_x = [R_x(x_1), \ldots, R_x(x_n)]^T = \hat{\mathbf{R}}_x / max\left(\hat{\mathbf{R}}_x\right) \quad (8)$$

where $R_x(x_i)$ will be called the "relevance coefficient (RC) of state x_i".

III. Microgrid modelling

Electronic DC/AC converters used as VSC are generally installed to interface RER in power systems. Within this technology, the main control structures for converters can be divided into grid-forming and grid-following. Grid-forming converters impose the voltage and frequency at their point of common coupling (PCC), and grid-following converters track the voltage and frequency of their PCC and orientate the current with respect to the voltage to meet the required injected active and reactive power. In this paper, we test the performance of the proposed algorithm in a microgrid based on the IEEE 69 bus distribution system [18] with seven grid-forming converters. Fig. 1 shows the control structure used for the converters, explained in [14]. The figure also includes the model used for the LCL output filter of the converter, with components L_f (inductance value of the converter-side inductor), C_f and L_c (inductance value of the grid-side inductor). Inductor models are completed with a series resistance R_f and R_c, and capacitors are modelled with a parallel resistance R_{cf}. The model is based on a d-q reference frame rotating with the frequency of one converter, and the switching and DC side of the converters are not included.

The different control layers included in Fig.1 are:

- Voltage and current controllers of each grid-forming converter ensure that the output voltage follows its set point with the aid of an inner control loop for the current through the converter side inductor. This control layer is often called 0-level control.
- The droop control, or primary control, stabilises the frequency after a disturbance and guarantees that all converters share the active-power change proportionally to their droop coefficient.
- The secondary control recovers the frequency and voltage to their nominal values after the primary control action. Here, we use the multi-agent secondary control presented in [19] and explained in [14]. With this multi-agent control structure, only one converter knows the set point for the system frequency (the so-called leader) and receives a voltage set point from external sources. All the other converters evolve cooperatively to a consensus solution with only the information of some "neighbour" converters.

IV. Case study

Table II includes the line and load data for the IEEE 69 bus distribution system presented in [18].

TABLE I
PARAMETERS USED FOR THE SIMULATION OF THE MICROGRID.

VCVSCs			
m_P	$1 \cdot 10^{-7}$ rad/s·W	n_Q	$1 \cdot 10^{-4}$ V/VAr
R_f	0.048 Ω	L_f	1.5 mH
C_f	66.32 μF	R_{cf}	48 $k\Omega$
R_c	0.048 Ω	L_c	1.5 mH
K_{PV}	0.02	K_{IV}	0.2
K_{PC}	50	K_{IC}	500
F_i	1	LPF_{const}	0.01 s
Sec. control parameters and bases			
c_f	1	c_v	1
f_{base}	50 Hz	S_{base}	3 MVA
delay (T_d)	0 s	$V_{nom} = V_{base}$	12.6 kV
β	0	B	1
$g_1 = 1$	$g_i = 0 \; \forall \; i \neq 1$	$a_{ij} = 1 \; \forall \; i \neq 1, \; j = i - 1$	
ω_{ref}	1 pu	v_{ref}	1 pu
Initial operation point ($i \in [1-7]$)			
P_i	532.54 kW	Q_i	374.82 kVAr

This system will be used as the case under study in this paper. The distribution system is operated islanded as a microgrid with seven grid-forming converters connected in the nodes shown in Table II.

TABLE II
IEEE 69-BUS SYSTEM DATA [18]. LOADS CONNECTED AT "TO" NODE. DGS CONNECTED AT "FROM" NODE.

from	to	R (Ω)	X (Ω)	P (kW)	Q (kVAr)	DGs
1	2	0.0005	0.0012	0	0	INV1
2	3	0.0005	0.0012	0	0	
3	4	0.0015	0.0036	0	0	
4	5	0.0251	0.0294	0	0	
5	6	0.366	0.1864	2.6	2.2	
6	7	0.3811	0.1941	40.4	30	
7	8	0.0922	0.047	75	54	
8	9	0.0493	0.0251	30	22	
9	10	0.819	0.2707	28	19	
10	11	0.1872	0.0619	145	104	
11	12	0.7114	0.2351	145	104	INV2
12	13	1.03	0.34	8	5.0	
13	14	1.044	0.345	8	5.5	
14	15	1.058	0.3496	0	0	
15	16	0.1966	0.065	45.5	30	
16	17	0.3744	0.1238	60	35	
17	18	0.0047	0.0016	60	35	
18	19	0.3276	0.1083	0	0	
19	20	0.2106	0.0696	1	0.6	
20	21	0.3416	0.1129	114	81	
21	22	0.014	0.0046	5.0	3.5	INV3
22	23	0.1591	0.0526	0	0	
23	24	0.3463	0.1145	28	20	
24	25	0.7488	0.2475	0	0	
25	26	0.3089	0.1021	14	10	
26	27	0.1732	0.0572	14	10	
3	28	0.0044	0.0108	26	18.6	
28	29	0.064	0.1565	26	18.6	
29	30	0.3978	0.1315	0	0	
30	31	0.0702	0.0232	0	0	
31	32	0.351	0.116	0	0	INV4
32	33	0.839	0.2816	14	10	
33	34	1.708	0.5646	19.5	14	
34	35	1.474	0.4873	6	4	
3	36	0.0044	0.0108	26	18.55	
36	37	0.0640	0.1565	26	18.55	
37	38	0.1053	0.1230	0.0	0.0	
38	39	0.0304	0.0355	24.0	17.0	
39	40	0.0018	0.0021	24.0	17.0	
40	41	0.7283	0.8509	1.2	1.0	
41	42	0.310	0.3623	0.00	0.0	INV5
42	43	0.041	0.0478	6.0	4	
43	44	0.0092	0.0116	0	0.0	
44	45	0.1089	0.1373	39	26	
45	46	0.00	0.0012	39	26	
4	47	0.0034	0.008	0	0	
47	48	0.0851	0.2083	79	56.4	
48	49	0.2898	0.7091	384.7	274.5	
49	50	0.0822	0.2011	384.7	274.5	
8	51	0.0928	0.0473	40.5	28.3	
51	52	0.332	0.1114	3.6	2.7	INV6
9	53	0.1740	0.0886	4.35	3.5	
53	54	0.203	0.1034	26.4	19	
54	55	0.2842	0.1447	24	17.2	
55	56	0.2813	0.1433	0	0	
56	57	1.5900	0.5337	0	0	
57	58	0.7837	0.2630	0	0	
58	59	0.3042	0.1006	100	72	
59	60	0.386	0.1172	0	0	
60	61	0.5075	0.259	1244	888	
61	62	0.0974	0.0496	32	23	INV7
62	63	0.1450	0.0738	0	0	
63	64	0.7105	0.3619	227	162	
64	65	1.04	0.5302	59	42	
11	66	0.201	0.0611	18	13	
66	67	0.0047	0.0014	18	13	
12	68	0.7394	0.2444	28	20	
68	69	0.0047	0.0016	28	20	

Table I shows the initial operating point for all simulations and linearisations and the parameters used for all the grid-forming converters. These parameters were chosen for a clear time-scale separation among control layers as the base case.

A. Performance of the algorithm in a case with clear time-scale separation

The microgrid described in Table II was modelled using Simulink® . All converters are equal, and their parameters are shown in Table I. The system is initialised and linearised

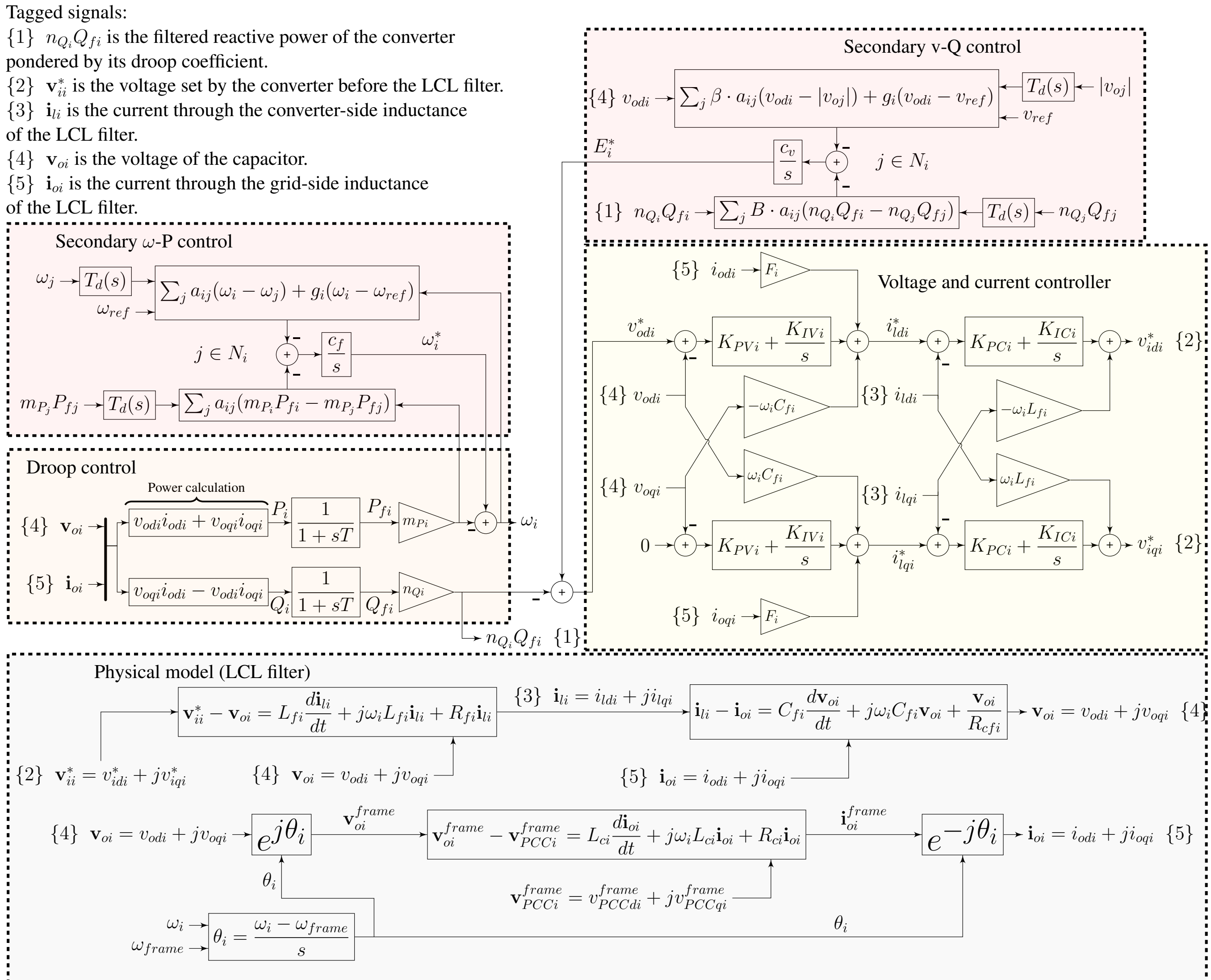

Fig. 1. Control diagram of one grid-forming converter modelled in d-q axes

using MATLAB® . The operating point used for linearisation is included in Table I.

Fig. 2 shows the state relevance data calculated using the algorithm described in Section II. States are grouped as described in Table III.

Fig. 2 shows that the most relevant dynamics are the secondary control and the frame calculation of all converters. The state relevance obtained suggests that eliminating the dynamics of all other variables will not significantly change the input-output response of the system.

Fig. 3 compares the time response of the complete and reduced models of the microgrid to a load change. The load change is defined as disconnecting the most significant load (node 61). Out of 337 state-space initial variables in the complete system, only 20 are considered in the reduced model, i.e. the reduced model is 94% smaller, reducing the computational burden. Fig. 3 confirms the conclusions drawn from the state relevance coefficient: the discarded states do not

TABLE III
NOMENCLATURE USED FOR THE GROUP OF STATES

Group	**Description**	**State order**
E^*	Secondary voltage control	1-7
LPF_P	Active power filter	1-7
LPF_Q	Reactive power filter	1-7
Lines	Line current	d-axis 1-68, q-axis 1-68
Loads	Load current	d-axis 1-48, q-axis 1-48
CC	Current controller	d-axis 1-7, q-axis 1-7
VC	Voltage controller	d-axis 1-7, q-axis 1-7
C_f	Filter capacitor voltage	d-axis 1-7, q-axis 1-7
L_c	Grid-side inductance current	d-axis 1-7, q-axis 1-7
L_f	Converter-side inductance current	d-axis 1-7, q-axis 1-7
ω^*	Secondary frequency control	1-7
frame	Calculation of reference frame	1-7
		Total: 337 States

contribute much to the system's dynamics.

B. Performance of the algorithm in a system close to its stability limit

In this case, we modify the parameters of the voltage controller of converter one (VSC_1) as given by (9).

$$K'_{pv} = 0.005K_{pv} \qquad\qquad K'_{iv} = 0.005K_{iv} \qquad (9)$$

This modification slows down VSC_1 voltage control, reducing the time-scale separation between the control layers of this converter and making the system lightly damped.

Fig. 4 shows the state relevance data calculated using the algorithm described in Section II. The figure shows that the most relevant dynamics are those of the secondary control, the frame calculation of all converters, and the voltage and current controller of VSC_1. Therefore, together with the reduced model, which considers instantaneous changes in power lines, loads, and voltage and current controllers (the conventional model reduction), we add to the comparison another reduced model that also includes the voltage and current controllers' dynamics of VSC_1, as suggested by the state relevance coefficient (see column bars *CC* and *VC* in Fig. 4).

Fig. 5 compares the time response of the complete model with two reduced ones to the same load change as in Section IV-A. The complete model has 337 states, the conventional reduced model has 20 states, and the reduction suggested by the state-relevance coefficient has 28 states. Notice that including the voltage and current controllers dynamics also involves the filter capacitor and converter-side inductance.

Results confirm the conclusions obtained with the state relevance coefficient: the discarded states do not contribute much to the system's dynamics, except for the voltage and current controller of VSC_1, which must be included to preserve a similar input-output response.

V. Conclusions

This paper analysed the performance of the algorithm presented to calculate the state relevance of a linear system in its input-output response when applied to a microgrid with 100% of its generation through grid-forming converters. It also explains the algorithm briefly and presents study cases to make it more understandable. Results clearly show the algorithm's performance, which can help quickly and precisely choose the most important states representing the system dynamics. If 0-level and secondary controls of a microgrid are designed with a clear difference in their time scales (a typical approach), the former is not very relevant in the studied input-output response. The state-relevance coefficient spots when the control of VSC_1 is slowed down through the increase of its 0-level control's relevance. Summarising, state relevance is not only affected by the physical parameters of the grid, but also by the operating point and the design of the various controllers which, naturally, affect the dynamics of the system.

References

[1] P. Kundur, N. J. Balu, and M. G. Lauby, *Power System Stability and Control*, ser. The EPRI Power System Engineering Series. New York: McGraw-Hill, 1994.

[2] H. Bevrani and J. Raisch, "On Virtual inertia Application in Power Grid Frequency Control," *Energy Procedia*, vol. 141, pp. 681–688, Dec. 2017.

[3] R. Eriksson, N. Modig, and K. Elkington, "Synthetic inertia versus fast frequency response: A definition," *IET Renewable Power Generation*, vol. 12, no. 5, pp. 507–514, Apr. 2018.

[4] S. Ghosh and N. Senroy, "A comparative study of two model order reduction approaches for application in power systems," in *2012 IEEE Power and Energy Society General Meeting*, Jul. 2012, pp. 1–8.

[5] T. Qoria, Q. Cossart, C. Li, X. Guillaud, F. Colas, F. Gruson, and X. Kestelyn, "WP3 - Control and Operation of a Grid with 100% Converter-Based Devices. Deliverable 3.2: Local control and simulation tools for large transmission systems," MIGRATE project, Tech. Rep., Dec. 2018, accessed 05/05/2022. [Online]. Available: https://www.h2020-migrate.eu/downloads.html

[6] J. Beerten, S. D'Arco, and J. A. Suul, "Frequency-dependent cable modelling for small-signal stability analysis of VSC-HVDC systems," *IET Generation, Transmission & Distribution*, vol. 10, no. 6, pp. 1370–1381, 2016.

[7] G. Grdenić, M. Delimar, and J. Beerten, "Assessment of AC network modeling impact on small-signal stability of AC systems with VSC HVDC converters," *International Journal of Electrical Power & Energy Systems*, vol. 119, p. 105897, 2020.

[8] C. Karawita and U. D. Annakkage, "A hybrid network model for small signal stability analysis of power systems," *IEEE Transactions on Power Systems*, vol. 25, no. 1, pp. 443–451, 2010.

[9] G. Grdenić, M. Delimar, and J. Beerten, "AC Grid Model Order Reduction Based on Interaction Modes Identification in Converter-Based Power Systems," *IEEE Transactions on Power Systems*, 2022.

[10] X. Wang and F. Blaabjerg, "Harmonic stability in power electronic-based power systems: Concept, modeling, and analysis," *IEEE Trans. Smart Grid.*, vol. 10, no. 3, pp. 2858–2870, 2019.

[11] A. Bayo Salas, "Control interactions in power systems with multiple VSC HVDC converters. Analysis, modelling and mitigation of electromagnetic stability problems," Ph.D. dissertation, Ph.D. Thesis / Arenberg Doctoral School, Faculty of Engineering Science, KU Leuven, 2018.

[12] A. Laub, M. Heath, C. Paige, and R. Ward, "Computation of system balancing transformations and other applications of simultaneous diagonalization algorithms," *IEEE Transactions on Automatic Control*, vol. 32, no. 2, pp. 115–122, Feb. 1987.

[13] A. Ramirez, A. Mehrizi-Sani, D. Hussein, M. Matar, M. Abdel-Rahman, J. Jesus Chavez, A. Davoudi, and S. Kamalasadan, "Application of Balanced Realizations for Model-Order Reduction of Dynamic Power System Equivalents," *IEEE Transactions on Power Delivery*, vol. 31, no. 5, pp. 2304–2312, Oct. 2016.

[14] A. Tomás-Martín, A. García-Cerrada, L. Sigrist, S. Yagüe, and J. Suárez-Porras, "State relevance and modal analysis in electrical microgrids with high penetration of electronic generation," *International Journal of Electrical Power & Energy Systems*, vol. 147, p. 108876, May 2023.

[15] B. Moore, "Principal component analysis in linear systems: Controllability, observability, and model reduction," *IEEE Transactions on Automatic Control*, vol. AC-26, no. 1, pp. 17–32, Feb. 1981.

[16] P. W. Sauer and M. A. Pai, *Power System Dynamics and Stability*. Upper Saddle River, N.J: Prentice Hall, 1998.

[17] I. Pérez-Arriaga, G. Verghese, and F. Schweppe, "Selective Modal Analysis with Applications to Electric Power Systems, PART I: Heuristic Introduction," *IEEE Transactions on Power Apparatus and Systems*, vol. PAS-101, no. 9, pp. 3117–3125, Sep. 1982.

[18] M. Baran and F. Wu, "Optimal capacitor placement on radial distribution systems," *IEEE Transactions on Power Delivery*, vol. 4, no. 1, pp. 725–734, Jan. 1989.

[19] A. Bidram, A. Davoudi, F. L. Lewis, and J. M. Guerrero, "Distributed Cooperative Secondary Control of Microgrids Using Feedback Linearization," *IEEE Transactions on Power Systems*, vol. 28, no. 3, pp. 3462–3470, Aug. 2013.

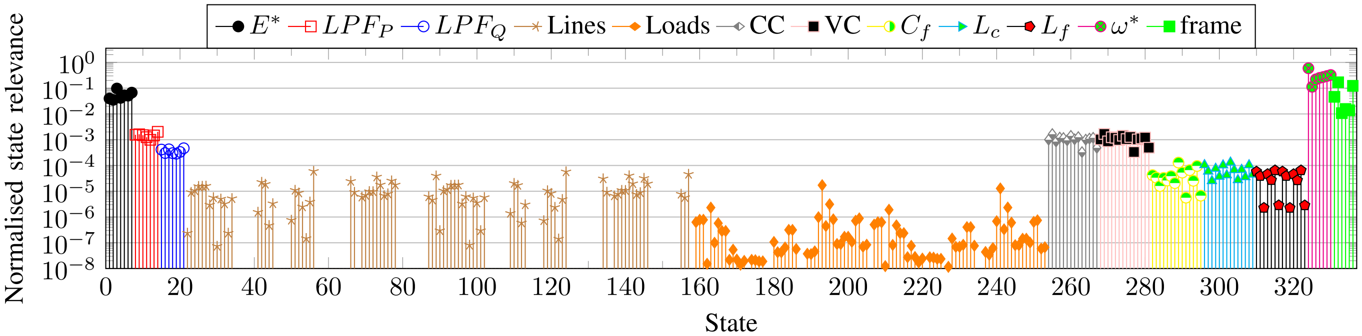

Fig. 2. Normalised state relevance of the base study case. Values below 10^{-8} are not shown for clarity.

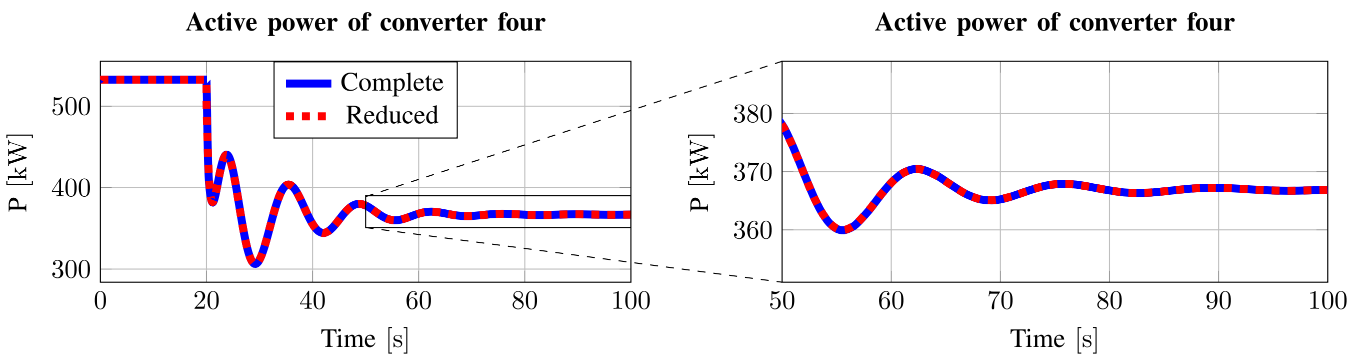

Fig. 3. Comparison of the time response of the complete and reduced models of the microgrid to a load change. The active power of inverter four VSC_4 is shown.

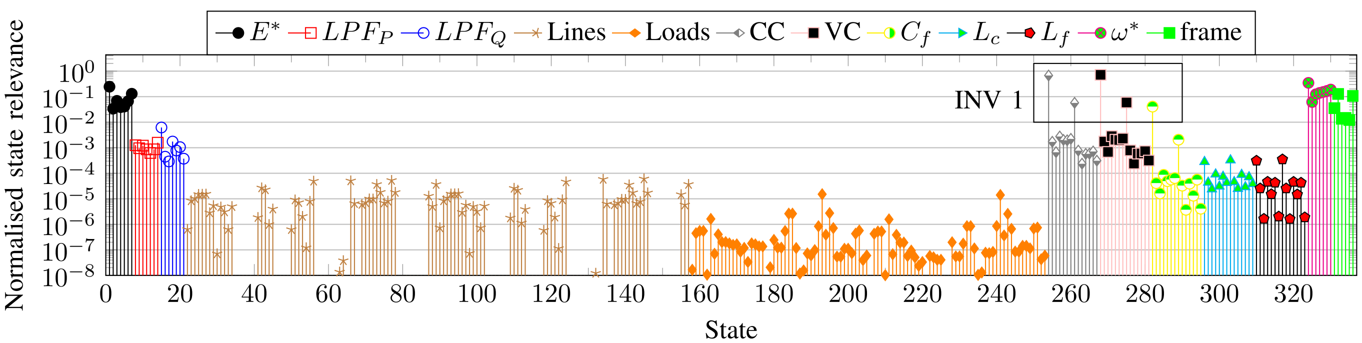

Fig. 4. Normalised state relevance of the study case with abnormal time-scale separation. Values below 10^{-8} are not shown for clarity.

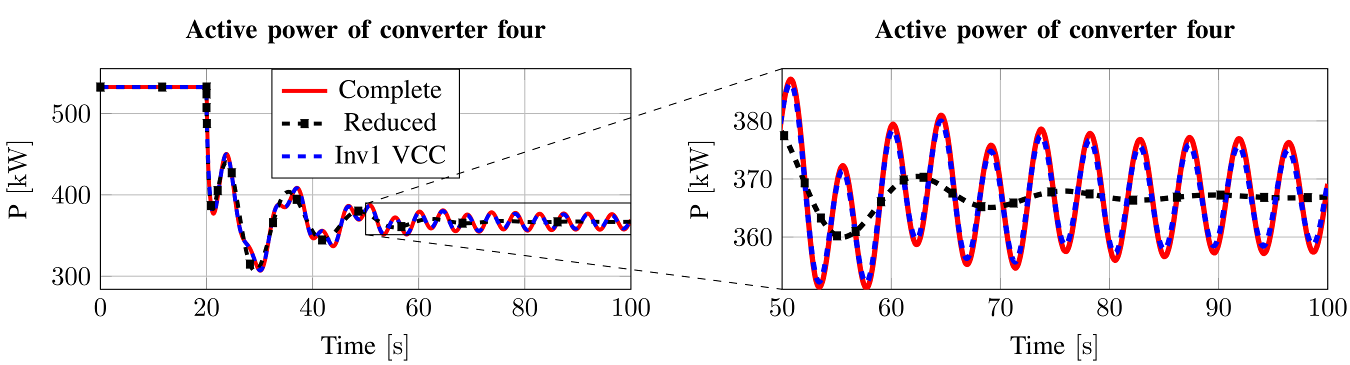

Fig. 5. Comparison of the time response of the complete and reduced models of the microgrid to a load change. The active power of VSC_4 is shown.